



### TO THE EDITOR:

# Natural history and cell of origin of *TCF3-ZNF384* and *PTPN11* mutations in monozygotic twins with concordant BCP-ALL

Clara Bueno,<sup>1,3,\*</sup> J. Ramón Tejedor,<sup>4,\*</sup> Rachael Bashford-Rogers,<sup>5,\*</sup> Laura González-Silva,<sup>6,\*</sup> Rafael Valdés-Mas,<sup>7</sup> Antonio Agraz-Doblás,<sup>1,3,6</sup> Rafael Díaz de la Guardia,<sup>1,2</sup> Jordi Ribera,<sup>1,2</sup> Lurdes Zamora,<sup>1,2</sup> Chrysteal Bilhou-Nabera,<sup>8,9</sup> Nassera Abermil,<sup>8,9</sup> Hélène Guermouche,<sup>8,9</sup> Elodie Gouache,<sup>10</sup> Guy Leverger,<sup>10</sup> Mario F. Fraga,<sup>11</sup> Agustín F. Fernández,<sup>4</sup> Paola Ballerini,<sup>8,†</sup> Ignacio Varela,<sup>6,†</sup> and Pablo Menendez<sup>1,3,12,†</sup>

<sup>1</sup>Josep Carreras Leukemia Research Institute, Barcelona, Spain; <sup>2</sup>Department of Biomedicine, School of Medicine, University of Barcelona, Barcelona, Spain; <sup>3</sup>Centro de Investigación Biomédica en Red de Cáncer, Instituto de Salud Carlos III, Barcelona, Spain; <sup>4</sup>Institute of Oncology of Asturias, Instituto de Investigación Sanitaria del Principado de Asturias, Hospital Universitario Central de Asturias, Oviedo, Spain; <sup>5</sup>Wellcome Centre for Human Genetics, University of Oxford, Oxford, United Kingdom; <sup>6</sup>Instituto de Biomedicina y Biotecnología de Cantabria, Universidad de Cantabria-CSIC, Santander, Spain; <sup>7</sup>Dreamgenics S.L., Oviedo, Spain; <sup>8</sup>Service d'Hématologie Biologique, Hospital Armand Trousseau, Paris, France; <sup>9</sup>Hématologie Biologique, Centre de Recherche Saint-Antoine, Hospital Saint-Antoine, Inserm, Sorbonne Université, Paris, France; <sup>10</sup>Department of Pediatric Hemato-oncology, Hospital Armand Trousseau, Paris, France; <sup>11</sup>Nanomaterials and Nanotechnology Research Center, Universidad de Oviedo, Oviedo, Spain; and <sup>12</sup>Institució Catalana de Recerca i Estudis Avançats, Barcelona, Spain

B-cell precursor acute lymphoblastic leukemia (BCP-ALL) is the most common childhood cancer and is molecularly heterogeneous.<sup>1</sup> Identical twins with concordant BCP-ALL have provided a unique and tractable model to delineate the natural history and clonal evolution of the disease.<sup>1-3</sup> Such studies have led to the 2-hit model for pediatric BCP-ALL, elucidated by Greaves,<sup>4</sup> which provides unambiguous evidence that an initiating alteration, often occurring in utero, generates a preleukemic clone, which eventually gives rise to an overt leukemia upon acquisition of secondary cooperating mutations.<sup>5</sup> Importantly, genome-wide sequencing has revealed a strikingly silent mutational landscape in childhood BCP-ALL, further indicative of a developmental cancer of prenatal origin, with a short window of time to accumulate molecular alterations.<sup>6-8</sup>

The natural history of the disease has been studied in major cytogenetic subgroups of childhood BCP-ALL, including MLL fusion,<sup>9-11</sup> ETV6-RUNX1<sup>+</sup>,<sup>12-14</sup> hyperdiploid,<sup>3,5,15,16</sup> BCR-ABL1<sup>+</sup>, and Ikaros mutated.<sup>17</sup> However, formal demonstration of the prenatal origin and backtracking of the natural history of the leukemia remain understudied in the major subgroup, so-called B-other ALL. This subgroup accounts for ~30% of de novo diagnoses and is defined by the absence of main classifying alterations (ie, chromosomal translocations, aneuploidy, and copy-number alterations and/or mutations recurrently observed in BCP-ALL), thus challenging the use of patient-specific molecular tags to backtrack the natural history of the disease.<sup>1,18-21</sup>

Predicated based on the hypothesis that shared identical mutations are prenatal in origin and twin-specific mutations are likely to be postnatal and secondary, we here performed a genome-wide multilayer OMICs analysis, including whole-genome DNA (WG-seq), B-cell receptor (BCR-seq), and whole-genome DNA bisulphite sequencing (WGB-seq) on a pair of 8-month-old monozygotic twins diagnosed with concordant B-other BCP-ALL. We demonstrate a parallel and convergent genetic and

epigenetic evolution of a *TCF3-ZNF384/PTPN11*-driven concordant B-other BCP-ALL and support a pre-VDJ primitive fetal hematopoietic progenitor or stem cell as the cell of origin of *TCF3-ZNF384* and *PTPN11* mutations.

Routine molecular diagnostics of monozygotic twins with concordant BCP-ALL revealed the absence of molecular/cytogenetic alterations associated with BCP-ALL (supplemental Table 1, available on the *Blood* Web site; supplemental Figure 1), thus classifying the leukemia as B-other BCP-ALL.<sup>8,20</sup> We therefore performed high-coverage WG-seq in purified blasts and peripheral blood cells at complete remission from both twins to comprehensively characterize the developmental timing of acquired somatic mutations (WG-seq detailed in supplemental Table 2). We found a total of 227 and 261 somatic mutations in twin A and twin B, respectively (Figure 1A; supplemental Table 3), which represents a low mutational load (~0.07 mutations per Mb) and is in line with the silent mutational landscape reported for infant BCP-ALL.<sup>6,7</sup> Notably, 75 somatic mutations were shared between both twins, suggesting a common prenatal origin of the leukemia (Figure 1A-B). Only 3 of these mutations affected coding regions: t(12;19)(p13;p13) encoding the *TCF3-ZNF384* fusion gene (Figure 1A; supplemental Figure 2A)<sup>22</sup> and point mutations in *SDAD1* and *UQCR11* (Figure 1B). These prenatal coding mutations showed a mutant allele frequency nearing 50%, thus representing initial events in the original leukemic clone. The t(12;19)(p13;p13)/*TCF3-ZNF384* rearrangement showed an identical genomic breakpoint in both twins (supplemental Figure 2A) and was confirmed by fluorescence in situ hybridization (supplemental Figure 2B) and RT-PCR (supplemental Figure 2C) and sequence validated (supplemental Figure 2D). The other coding mutations were validated using orthogonal sequencing strategies (supplemental Table 4).

We additionally found 152 and 186 somatic mutations exclusive to twin A and twin B, respectively, suggesting that, during

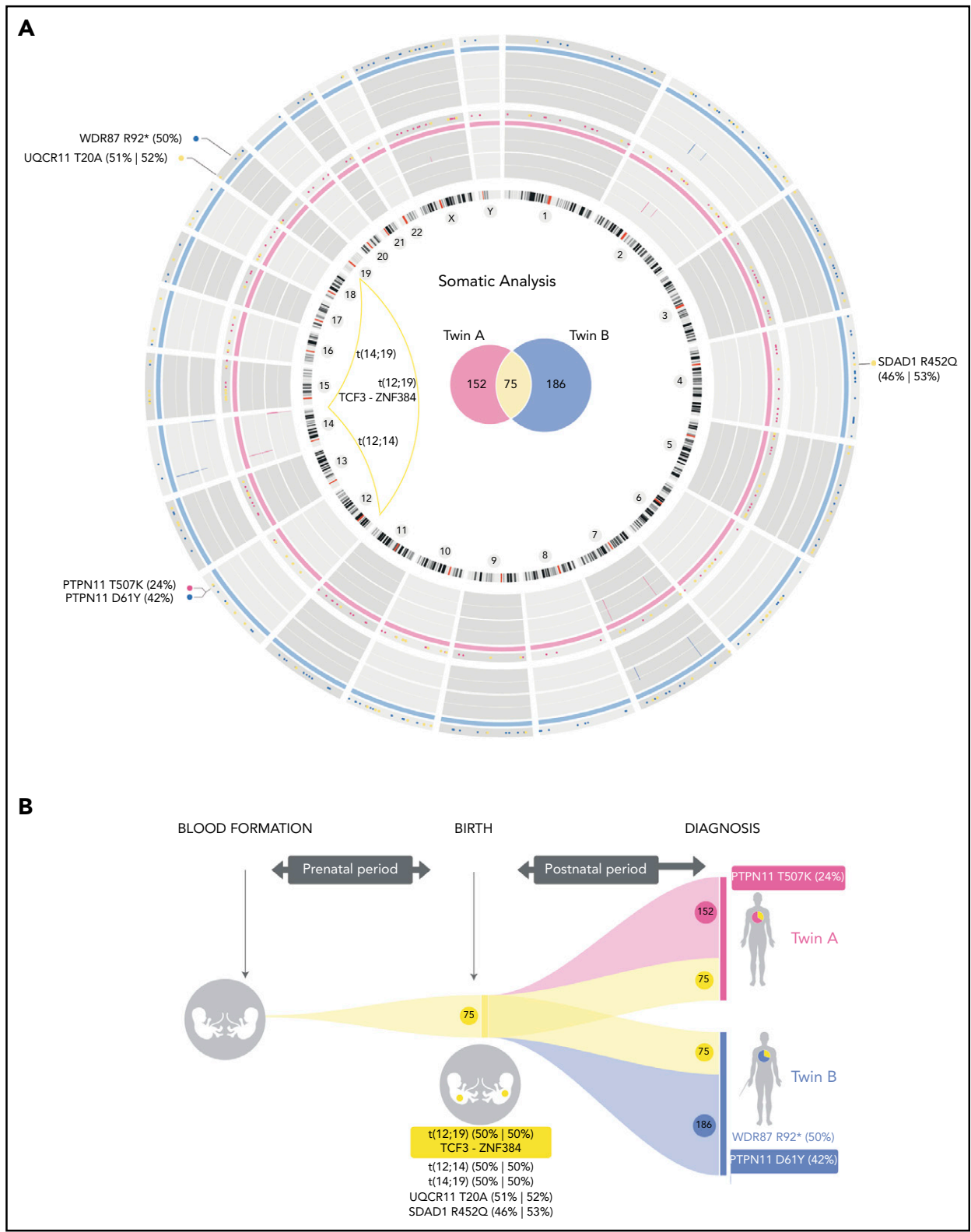


**Figure 1. Mutational landscape and natural history reconstruction of BCP-ALL monozygotic twins.** (A) Circos plot (<http://circos.ca/>) representing the total number of mutations identified at diagnosis for each twin. Twin A is shown in pink (inner ring). Twin B is shown in blue (outer ring). Chromosome ideograms are indicated inside the graph. Copy-number alterations are represented as lines within the gray rings. Venn diagrams inside the graph show the total number of exclusive (pink, twin A; blue, twin B) and shared (yellow) somatic mutations. Coding mutations are annotated outside the graph according to genomic gene location. Substitution mutant allele frequency is shown in brackets. Genomic chromosomal rearrangements are represented with yellow lines connecting chromosomal breakpoints. (B) Graphical reconstruction of the number of mutations accumulated during tumor history. Approximately one-third of the somatic mutations (shown in yellow), including the translocation responsible for the expression of the TCF3-ZNF384 fusion gene, occurred before birth, when both twins shared the same circulatory system. Coding mutations are indicated. Leukemia in both twins evolved independently after birth, with twin-specific postnatal mutations.

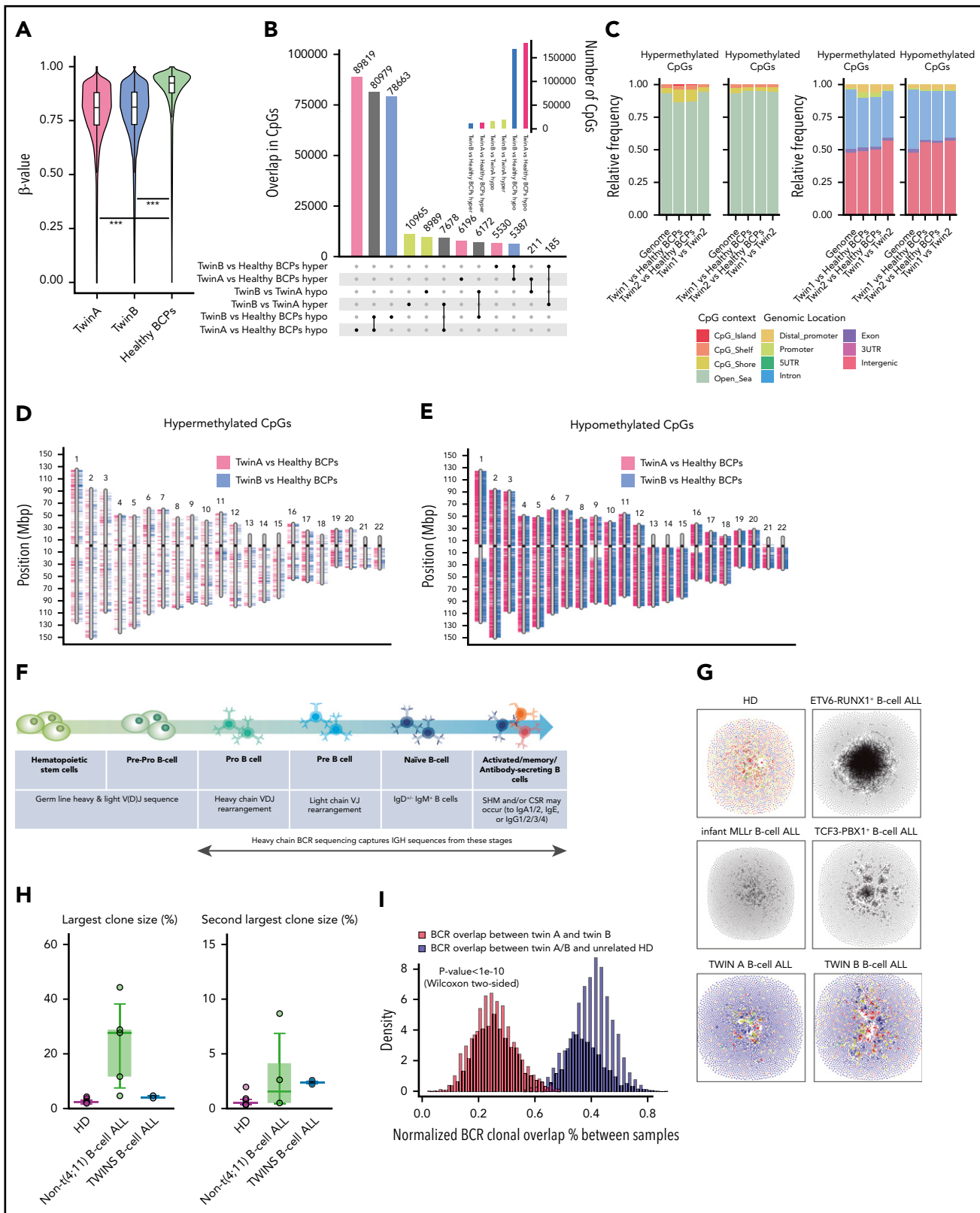


**Figure 2. Genome-wide DNA methylation analysis and BCR repertoires in BCP-ALL monozygotic twins.** (A) Violin plots depicting the global DNA methylation levels ( $\beta$ -value distributions) of CpG sites identified by WGB-seq. For healthy BCPs, the average DNA methylation value of 2 FL-derived pools of BCP is represented. (B) Total number of differentially hyper- (hyper) and hypomethylated (hypo) CpGs observed for the indicated comparisons between twins and healthy BCPs. The inner graph represents the total number of differentially methylated CpG (dmCpG) sites. (C) Stacked bar plots indicating the relative proportion of significant hyper- and hypomethylated CpGs between twins, or between each twin and healthy BCPs, regarding their CpG context (left) or the CpG genomic location (right), respectively, as indicated in the colored legend. (D-E) Ideograms representing the genomic location of differentially DNA hypermethylated (D) and hypomethylated (E) CpG sites obtained for twin A (pink) and twin B (blue) as compared with healthy BCPs. (F) Cartoon summarizing how BCR-seq captures IgH sequences from these stages. (G) Network plots of BCR repertoires of a representative healthy

individual development, the leukemias evolved in parallel, and twin-specific mutations accumulated postnatally (Figure 1A-B; supplemental Table 3). Regarding coding mutations, each twin acquired a distinct nonsynonymous mutation in *PTPN11*<sup>23</sup> (Figure 1A-B; supplemental Figure 3). Both coding mutations in *PTPN11* were subclonal and predicted by SHIFT and POLYPHEN algorithms to affect evolutionary conserved amino acids and significantly affect the function of the protein domains involved. The 2 identified mutations (D61Y and T507K) affect domains that modulate PTPN11 phosphatase activity, previously described to increase PTPN11 activity. Therefore, these *PTPN11* mutations likely represent gain-of-function postnatal secondary oncogenic hits, promoting proliferation and cooperating with *TCF3-ZNF384* for overt leukemia development, suggesting a convergent evolution in both leukemias.

To further explore the evolutionary traits of the concordant BCP-ALL in both twins, we used WGB-seq to survey the DNA methylation status of concordant BCP-ALLs (WGB-seq detailed in supplemental Table 5). BCP-ALL cells from both twins were significantly hypomethylated as compared with their healthy FL-BCP counterparts (Figure 2A). In fact, among the ~190 000 and ~176 000 dmCpG sites found for twin A and B, respectively, the number of hypomethylated CpG sites largely outperformed the number of hypermethylated sites (Figure 2B). However, we observed limited DNA methylation changes between the twins' leukemic cells (Figure 2B green bars). Indeed, both twins displayed a similar enrichment of dmCpG sites, both hyper- and hypomethylated, with regard to their CpG context (Figure 2C) or CpG genomic location (Figure 2C-E). The relatively few dmCpG sites observed between twins might reflect interindividual variability rather than a divergent epigenetic evolution of the leukemia, reinforcing a parallel and convergent genetic, but also epigenetic, evolution of the BCP-ALL in this pair of monozygotic twins.

Whether pathogenic chromosomal rearrangements and/or protein-coding DNA mutations in cancer are associated with chromatin and/or DNA methylation changes remains elusive. We therefore wanted to gain insight into the methylation status of the loci specifically found rearranged or mutated in both twins (*TCF3*, *ZNF384*, *SDAD1*, *UQCR11*, *WRD87*, and *PTPN11*). Strikingly, in contrast to healthy FL-BCPs and BCP-ALL cells from unrelated infant B-other ALLs, we found that BCP-ALL cells from both twins displayed concordant and specific significant DNA hypomethylation in *TCF3* and *ZNF384* loci, in the vicinity of the translocation genomic breakpoints (supplemental Figure 4A-B), but also within the promoter or body gene region of *SDAD1*, *WRD87*, and *PTPN11*, coinciding with CpG islands and shore regions (supplemental Figure 4C-F). Importantly, DNA methylation changes were not observed in *MLL* or *TP53* loci (supplemental Figure 4G-H), supporting the specificity of the DNA hypomethylation observed in the loci rearranged/mutated in leukemic twins.

We next analyzed BCR repertoires to study the clonal composition of immunoglobulin heavy chain (IgH) rearrangements in

diagnostic samples from both twins. BCRs are generated during B-cell differentiation (Figure 2F) and represent unique molecular tags for each B-cell clone through the recombination of V, D, and J genes, thus providing a detailed view of the B-cell population dynamics and clone tracking.<sup>6,24</sup> We therefore performed BCR-seq on *TCF3-ZNF384*<sup>+</sup> BCP-ALL cells from both twins to address whether they expressed fully rearranged BCRs, from which major B-cell clonal expansion may be observed.<sup>6,24</sup> After BCR-seq filtering, each sample yielded 6362 and 11 832 unique BCRs for twin A and B, respectively. Similar to that reported for infant mixed-lineage leukemia–rearranged pro-B ALL, BCR repertoires from infant *TCF3-ZNF384*<sup>+</sup> BCP-ALL twins did not exhibit significantly expanded VDJ-rearranged B-cell clones (Figure 2G-H). This is in contrast to the significantly large B-cell clones consistently observed in noninfant *t(1;19)/TCF3-PBX1*<sup>+</sup>, *t(12;21)/ETV6-RUNX1*<sup>+</sup>, and *t(9;22)/BCR-ABL1*<sup>+</sup> BCP-ALLs.

Because the *TCF3-ZNF384*, *SDAD1*, and *UQCR11* mutations are clonal, and *PTPN11* mutations are found in major clones, the lack of B-cell clonal expansion based on IgH rearrangements, together with the leukemia phenotype developmentally stalled at the pro-B stage, supports a model in which the genomic drivers in this pair of infant leukemic twins originate in a primitive fetal progenitor with a germ line or an incompletely rearranged (pre-VDJ) IgH locus.<sup>6</sup> The fifth Ewing variant transcription factor is uniquely expressed in fetal primitive hematopoietic stem and progenitor cells and has been shown to be expressed on a vast majority of infant leukemias with a prenatal origin.<sup>25</sup> Through a diagnostic approach, we confirmed a significantly higher expression of fifth Ewing variant transcription factor in both leukemic twins and infant/pediatric B-ALLs (*n* = 11) than in adult B-ALLs (*n* = 5), further supporting the primitive fetal progenitor nature of the cell of origin in both leukemic twins (supplemental Figure 5). Given that IgH rearrangement is a highly epigenetically regulated process, we would predict a higher similarity of VDJ rearrangements between the twins, given their shared mutations and epigenetic landscapes. Indeed, the BCR clonal overlap between the twins was threefold higher than that between twins and healthy donors (Figure 2I). The shared IgH sequences between the twins comprised multiple small clones, primarily IgD/M, with a strong concordance of isotype usage between the twins (supplemental Figure 6). Together, these data demonstrate the concordance between B-cell populations in both infant twins, consistent with shared epigenetic landscapes of B-cell progenitor populations.

Finally, bone marrow–derived mesenchymal stem cells (BM-MSCs) play a role in the pathogenesis of a variety of hematological malignancies,<sup>26</sup> and leukemia-specific genetic alterations have been found in BM-MSCs from *MLL*-rearranged infant BCP-ALL patients, indicating that stromal cells may be in part tumor related and that such oncogenic insults may arise in a population of prehematopoietic precursors.<sup>27,28</sup> To further ascertain the cellular origin of the coding mutations found in our leukemic twins, we

**Figure 2 (continued)** donor (HD) and an infant mixed-lineage leukemia–rearranged (rMLL) pro-B ALL depicting the existence of many minor diagnostic nonexpanded B-cell clones (top middle left). Network plots of BCR repertoires of a representative *t(12;21)/ETV6-RUNX1*<sup>+</sup> and *t(1;19)/TCF3-PBX1*<sup>+</sup> pediatric BCP-ALL showing high clonality of B-cell clones (top middle right). Network plots of BCR repertoires of *TCF3-ZNF384*-rearranged pro-B ALL in both monozygotic twins (bottom). Each vertex represents a unique BCR sequence, and relative vertex size is proportional to the number of identical reads. For the HD and BCP-ALL twin samples, each vertex is represented by a pie chart indicating the percentage of each isotype, where blue = IgD/M, red = IgA1/2, yellow = IgG1/2, green = IgG3, and gray = IgE. (H) Boxplots of the largest and second largest BCR clone sizes for HD, non-*t(4;11)*<sup>+</sup> BCP-ALL, and twins with concordant BCP-ALL. (I) Histogram representing the number of BCR clones shared between twin A and twin B (blue) or between unrelated HD and the twins (red).

generated and characterized bona fide BM-MSCs cultures<sup>29</sup> and used fluorescence in situ hybridization and targeted sequencing to search for the presence of both shared and twin-specific coding mutations found in the leukemic cells. Such coding mutations were not detected in BM-MSCs from either twin, suggesting that BM-MSCs do not seem to be tumor related in these leukemic twins. This further confirms that both shared and twin-specific coding mutations arise in an early hematopoietic fetal pre-VDJ progenitor or stem cell, rather than in prehematopoietic precursors, and provides insight into the timing of these mutations. In sum, this is the first report on the natural history, evolutionary trajectories, and cell of origin of *TCF3-ZNF384* and *PTPN11* mutations in a pair of infant monozygotic twins with concordant B-other BCP-ALL. WG-seq and WGB-seq data sets have been deposited in the European Genome-Phenome Archive under the accession numbers EGAD00001005017 and EGAD00001005018, respectively. Data access will be granted upon request.

## Acknowledgments

The authors thank Mireia Camos (Hospital Sant Joan de Déu Barcelona, Barcelona, Spain) for critical reading of the manuscript.

This work was supported by European Research Council grants CoG-2014-646903 and PoC-2018-811220 (P.M.) and StG-2014-637904 (I.V.), Generalitat de Catalunya grants SGR330 and PERIS 2017-2019 (P.M.), Spanish Ministry of Economy and Competitiveness grants SAF2016-80481-R and SAF2016-76758-R (P.M. and I.V.), Spanish Association Against Cancer grant AECC-CI-2015 (C.B.), Health Institute Carlos III grant PI17/01028 (C.B.), and a FERO Foundation grant (C.B.). P.M. also acknowledges financial support from the Obra Social La Caixa-Fundació Josep Carreras and Fundación Leo Messi. J.R.T. is supported by a Juan de la Cierva Formación fellowship from the Spanish Ministry of Science and Innovation (FJCI-2015-26965) and Institute of Oncology of Asturias. R.V.-M. is supported by a Torres Quevedo fellowship from the Spanish Ministry of Science and Innovation (PTQ-16-08623). P.M. is an investigator of the Spanish Cell Therapy Cooperative Network.

## Authorship

Contribution: C.B., J.R.T., R.B.-R., L.G.-S., R.V.-M., A.A.-D., R.D.d.I.G., J.R., and L.Z. performed experiments and analyzed data; C.B., A.F.F., M.F.F., C.B.-N., N.A., H.G., E.G., G.L., P.B., I.V., and P.M. conceived the study, designed experiments, and analyzed data; and C.B., J.R.T., R.B.-R., R.V.-M., L.G.-S., I.V., and P.M. contributed to artwork and wrote the manuscript.

Conflict-of-interest disclosure: The authors declare no competing financial interests.

ORCID profiles: H.G., 0000-0003-4074-1623; A.F.F., 0000-0002-3792-4085.

Correspondence: Paola Ballerini, Service d'Hématologie Biologique, Hospital Armand Trousseau, Paris, France; e-mail: paola.ballerini@aphp.fr; Ignacio Varela, Instituto de Biomedicina y Biotecnología de Cantabria, Universidad de Cantabria-CSIC, Santander, Spain; e-mail: ignacio.varela@unican.es; and Pablo Menendez, Josep Carreras Leukemia Research Institute, School of Medicine, University of Barcelona, Casanova 143, 08036 Barcelona, Spain; e-mail: pmenendez@carrerasresearch.org.

## Footnotes

\*C.B., J.R.T., R.B.-R., and L.G.-S. contributed equally as first authors.

†P.B., I.V., and P.M. contributed equally as senior authors.

The online version of this article contains a data supplement.

## REFERENCES

- Hunger SP, Mullighan CG. Redefining ALL classification: toward detecting high-risk ALL and implementing precision medicine. *Blood*. 2015;125(26):3977-3987.
- Greaves MF, Maia AT, Wiemels JL, Ford AM. Leukemia in twins: lessons in natural history. *Blood*. 2003;102(7):2321-2333.
- Maia AT, Koehling J, Corbett R, Metzler M, Wiemels JL, Greaves M. Protracted postnatal natural histories in childhood leukemia. *Genes Chromosomes Cancer*. 2004;39(4):335-340.
- Greaves M. Molecular genetics, natural history and the demise of childhood leukaemia. *Eur J Cancer*. 1999;35(14):1941-1953.
- Bateman CM, Colman SM, Chaplin T, et al. Acquisition of genome-wide copy number alterations in monozygotic twins with acute lymphoblastic leukemia. *Blood*. 2010;115(17):3553-3558.
- Agraz-Doblas A, Bueno C, Bashford-Rogers R, et al. Unraveling the cellular origin and clinical prognostic markers of infant B-cell acute lymphoblastic leukemia using genome-wide analysis. *Haematologica*. 2019;104(6):1176-1188.
- Anderson K, Lutz C, van Delft FW, et al. Genetic variegation of clonal architecture and propagating cells in leukaemia. *Nature*. 2011;469(7330):356-361.
- Mullighan CG. The genomic landscape of acute lymphoblastic leukemia in children and young adults. *Hematology Am Soc Hematol Educ Program*. 2014;2014:174-180.
- Ford AM, Bennett CA, Price CM, Bruin MC, Van Wering ER, Greaves M. Fetal origins of the TEL-AML1 fusion gene in identical twins with leukemia. *Proc Natl Acad Sci USA*. 1998;95(8):4584-4588.
- Sanjuan-Pla A, Bueno C, Prieto C, et al. Revisiting the biology of infant t(4;11)/MLL-AF4+ B-cell acute lymphoblastic leukemia. *Blood*. 2015;126(25):2676-2685.
- Urtishak KA, Robinson BW, Rappaport EF, et al. Unique familial MLL(KMT2A)-rearranged precursor B-cell infant acute lymphoblastic leukemia in non-twin siblings. *Pediatr Blood Cancer*. 2016;63(7):1175-1180.
- Alpar D, Wren D, Ermini L, et al. Clonal origins of ETV6-RUNX1+ acute lymphoblastic leukemia: studies in monozygotic twins. *Leukemia*. 2015;29(4):839-846.
- Bungaro S, Irving J, Tussiwand R, et al. Genomic analysis of different clonal evolution in a twin pair with t(12;21) positive acute lymphoblastic leukemia sharing the same prenatal clone. *Leukemia*. 2008;22(1):208-211.
- Wiemels JL, Ford AM, Van Wering ER, Postma A, Greaves M. Protracted and variable latency of acute lymphoblastic leukemia after TEL-AML1 gene fusion in utero. *Blood*. 1999;94(3):1057-1062.
- Maia AT, Tussiwand R, Cazzaniga G, et al. Identification of preleukemic precursors of hyperdiploid acute lymphoblastic leukemia in cord blood. *Genes Chromosomes Cancer*. 2004;40(1):38-43.
- Maia AT, van der Velden VH, Harrison CJ, et al. Prenatal origin of hyperdiploid acute lymphoblastic leukemia in identical twins. *Leukemia*. 2003;17(11):2202-2206.
- Cazzaniga G, van Delft FW, Lo Nigro L, et al. Developmental origins and impact of BCR-ABL1 fusion and IKZF1 deletions in monozygotic twins with Ph+ acute lymphoblastic leukemia. *Blood*. 2011;118(20):5559-5564.
- Galbati M, Lettieri A, Micalizzi C, et al. Natural history of acute lymphoblastic leukemia in neurofibromatosis type 1 monozygotic twins. *Leukemia*. 2013;27(8):1778-1781.
- Ma Y, Dobbins SE, Sherborne AL, et al. Developmental timing of mutations revealed by whole-genome sequencing of twins with acute lymphoblastic leukemia. *Proc Natl Acad Sci USA*. 2013;110(18):7429-7433.
- Moorman AV. New and emerging prognostic and predictive genetic biomarkers in B-cell precursor acute lymphoblastic leukemia. *Haematologica*. 2016;101(4):407-416.
- Zaliova M, Stuchly J, Winkowska L, et al. Genomic landscape of pediatric B-other acute lymphoblastic leukemia in a consecutive European cohort. *Haematologica*. 2019;104(7):1396-1406.

22. Hirabayashi S, Ohki K, Nakabayashi K, et al; Tokyo Children's Cancer Study Group (TCCSG). ZNF384-related fusion genes define a subgroup of childhood B-cell precursor acute lymphoblastic leukemia with a characteristic immunotype. *Haematologica*. 2017;102(1):118-129.
23. Molteni CG, Te Kronnie G, Biciato S, et al. PTPN11 mutations in childhood acute lymphoblastic leukemia occur as a secondary event associated with high hyperdiploidy. *Leukemia*. 2010;24(1):232-235.
24. Bashford-Rogers RJ, Nicolaou KA, Bartram J, et al. Eye on the B-ALL: B-cell receptor repertoires reveal persistence of numerous B-lymphoblastic leukemia subclones from diagnosis to relapse. *Leukemia*. 2016;30(12):2312-2321.
25. Liu TH, Tang YJ, Huang Y, et al. Expression of the fetal hematopoiesis regulator FEV indicates leukemias of prenatal origin. *Leukemia*. 2017;31(5):1079-1086.
26. García-Castro J, Trigueros C, Madrenas J, Pérez-Simón JA, Rodríguez R, Menendez P. Mesenchymal stem cells and their use as cell replacement therapy and disease modelling tool. *J Cell Mol Med*. 2008;12(6B):2552-2565.
27. Menendez P, Catalina P, Rodríguez R, et al. Bone marrow mesenchymal stem cells from infants with MLL-AF4+ acute leukemia harbor and express the MLL-AF4 fusion gene. *J Exp Med*. 2009;206(13):3131-3141.
28. Shalapour S, Eckert C, Seeger K, et al. Leukemia-associated genetic aberrations in mesenchymal stem cells of children with acute lymphoblastic leukemia. *J Mol Med (Berl)*. 2010;88(3):249-265.
29. Diaz de la Guardia R, Lopez-Millan B, Lavoie JR, et al. Detailed characterization of mesenchymal stem/stromal cells from a large cohort of AML patients demonstrates a definitive link to treatment outcomes. *Stem Cell Reports*. 2017;8(6):1573-1586.

DOI 10.1182/blood.2019000893

© 2019 by The American Society of Hematology